

Experimental analysis of wind action on a large wavy roofing

Andrea Imbrenda¹, Marco Graziosi¹, Aymane Graini¹, Tommaso Massai²,
Gianni Bartoli², Claudio Mannini²

¹*PROGES ENGINEERING S.r.l, Rome, Italy, a.imbrenda@progesengineering.com;*

²*Department of Civil and Environmental Engineering, University of Florence, Florence, Italy,
tommaso.massai@unifi.it; gianni.bartoli@unifi.it; claudio.mannini@unifi.it*

SUMMARY:

Wind-induced pressure field on a large wavy roofing supported by a spatial lattice structure and covering the new passenger terminal at Rabat Airport (Morocco) was experimentally investigated at the CRIACIV Wind Tunnel Laboratory in Prato, Italy. This double-curved roofing has a plan projection size of 265×115 m² and a maximum height of 41.5 m, and was reproduced in the wind tunnel at a scale 1:300. The extensive experimental study is mainly due to the peculiar shape of the roofing, whose aerodynamics is obviously not covered by codes or reference literature. The tests were aimed at determining pressure coefficients and associated resultant forces. A large number of simultaneous time histories of external and net pressure coefficients were recorded all over the roofing structure, and the data were statistically analysed to obtain both mean and local peak values. The results were then processed through a well-established and computationally efficient frequency-domain procedure to determine the expected static and dynamic stresses in the lattice structure and the values of support reactions.

Keywords: double-curved roofing, wind tunnel tests, dynamic structural response

1. INTRODUCTION

Airport terminals are a rather widespread and specific structural type, having strong social and economic impacts. Their principal scope is to cover a vast area, so that structural design issues and pronounced sensitivity to wind effects (due to the extremely large exposed surface and the low incidence of dead loads) are intrinsic characteristics, making them a natural link between research and technological applications.

Codes and standards cannot take into account all possible architectural solutions: indeed, complex geometries assume their major expressions, with countless variants and enterprising design, for large covering systems. Then, avoiding numerical approaches, which need to be in any case validated, experimental measurements are still the best solution for pressure field quantification.

In the current work, the results of a broad wind tunnel study on the large double-curvature wavy roofing of the new passenger terminal at Rabat Airport, Morocco (Fig. 1), are presented and discussed. Then, the measured loads are employed to efficiently calculate in the frequency-domain the peak values of the internal forces in the elements that compose the spatial lattice structure supporting the roofing and the extreme values of the support reactions.

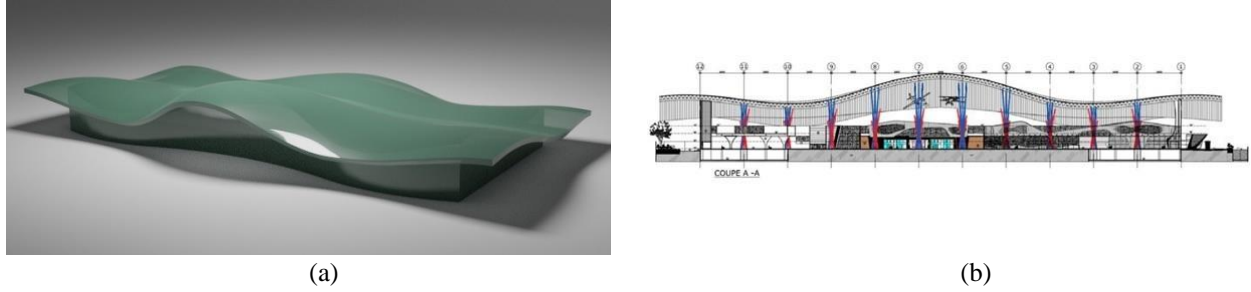


Figure 1. Terminal geometry: (a) 3D render, and (b) longitudinal section.

2. WIND TUNNEL SET-UP

2.1. Wind characteristics

The experimental campaign was carried out at the CRIACIV wind tunnel (Prato, Italy), which presents an 11 m-long test chamber with a section $2.4 \times 1.6 \text{ m}^2$. The atmospheric boundary layer reproduced in the wind tunnel was tuned by means of numerous preliminary analyses to obtain a wind profile targeting that provided by Eurocode 1 for the terrain category II (EN 1991-1-4, 2010). The mean flow velocity and longitudinal turbulence intensity as a function of the height above the ground are shown in Figure 2.

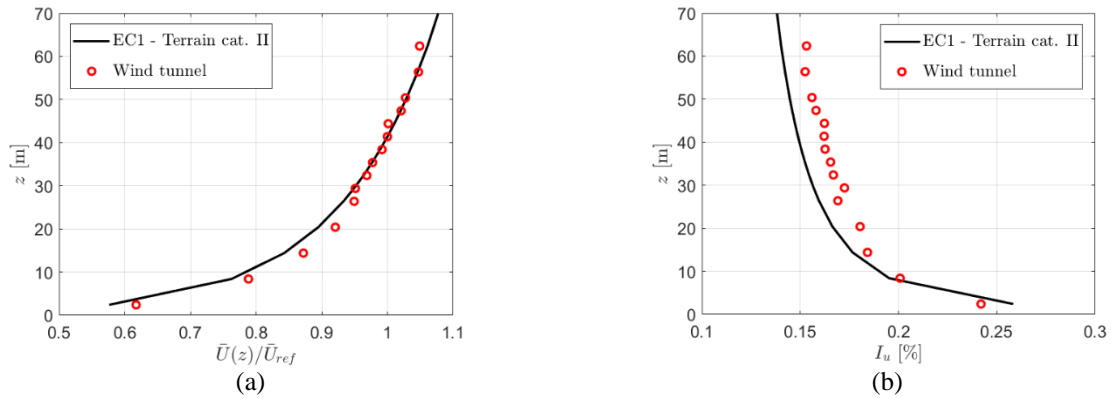


Figure 2. (a) Mean velocity profile normalized with the value at the roofing top; (b) turbulence intensity wind profile. The height z above the ground is reported at prototype scale.

2.2. Model

The new terminal at Rabat Airport occupies an area of $265 \times 115 \text{ m}^2$ and presents a maximum height above the ground of 41.5 m. Its wind tunnel model was realized at the scale 1:300. The curved main façade of the building and the roofing were 3D-printed using a special hard wax, while the other external walls of the terminal were made of wooden cardboard. The building of the old airport terminal was also reproduced on the wind tunnel turntable. The scale of the model was chosen based on the abovementioned wind profile reproduced in the wind tunnel and allows a sufficiently large Reynolds number. However, tests were carried out for three wind speeds to detect possible Reynolds number effects, namely 15, 20 and 25 m/s at the roofing top height, corresponding to velocity scales 1:0.41, 1:0.55 and 1:0.69, respectively. 191 pressure taps were installed all over the roofing external surface (Fig. 3(a)), mostly in the middle points of the $24 \times 24 \text{ m}^2$ square portions of the plan projection defined by the columns supporting the structure. Nevertheless, in the external

portion of the roofing jutting out of the terminal façades, pressure taps were placed both on the upper and on the lower surface, so to be able to measure net pressures on the projecting roof. Pressures were simultaneously recorded at a rate of 500 Hz with the system PSI DTC Initium.

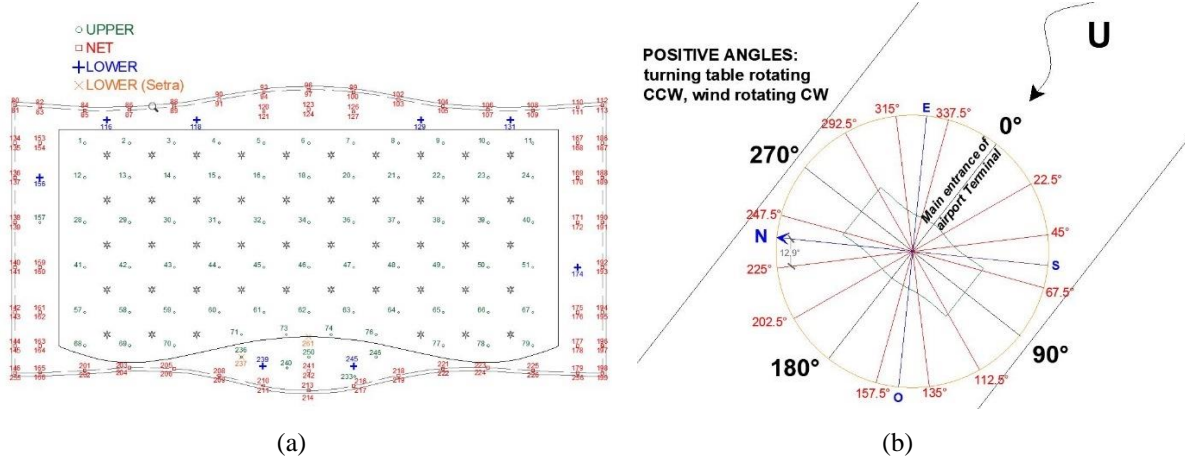


Figure 3. Pressure tap distribution over the wind tunnel model (a) and wind directions considered (b).

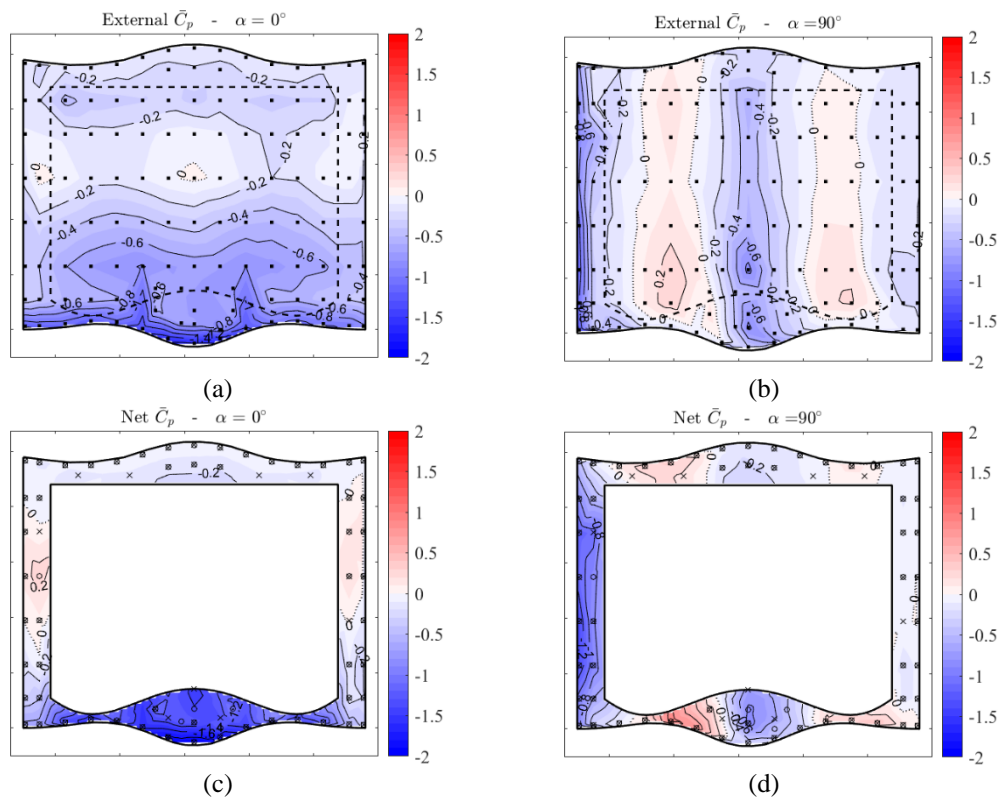


Figure 4. Examples of mean pressure coefficient maps: a) external pressure, $\alpha = 0^\circ$; b) external pressure, $\alpha = 90^\circ$; c) net pressure, $\alpha = 0^\circ$; d) net pressure, $\alpha = 90^\circ$. The wind tunnel reference mean wind is 19.7 m/s.

3. EXPERIMENTAL RESULTS

Mean, standard deviation and expected maximum and minimum pressure coefficients were determined for each time history recorded. Extreme value analysis was conducted using Cook and

Mayne approach (Cook and Mayne, 1980) assuming a Gumbel distribution of pressure peak values. The important issue of area averaging was dealt with through 1 s and 3 s-moving averages of the recorded pressure time histories prior to calculating the peak values (see, e.g., Lawson, 1976). Tests were repeated for 16 wind directions, every 22.5°, starting from the direction perpendicular to the main facade ($\alpha = 0^\circ$, see Figure 3(b)). Pressure coefficients were normalized with the mean wind velocity pressure at the reference height corresponding to the roofing top (41.5 m in prototype scale, 13 cm in model scale). Examples of pressure coefficient maps obtained are shown in Fig. 4. The complicated pressure pattern due to the wavy geometry of the roofing is apparent (see, e.g., Fig. 4(b) and 4(d)), along with the large lifting force acting on the cantilever portion of the roofing above the main entrance of the terminal, which is crucial for the structural design.

4. STRUCTURAL DYNAMIC RESPONSE

Structural response is obtained in the frequency domain assuming that the fluctuating part of wind loads can be characterized as Gaussian random processes. Only the peak value of members' internal forces is here of concern to design the inner lattice structure supporting the roofing surface. Denoting as x the generic response displacement, its peak value is expressed as $x^{min} = g^{min}\sigma_x$ and $x^{max} = g^{max}\sigma_x$, where g and σ_x are the peak factor and the standard deviation, respectively. The general equation of motion $\mathbf{M}\ddot{\mathbf{x}}(t) + \mathbf{C}\dot{\mathbf{x}}(t) + \mathbf{K}\mathbf{x}(t) = \mathbf{f}(t)$ can be expressed using the Fourier transform as $\mathbf{G} \cdot \hat{\mathbf{x}} = \hat{\mathbf{f}}$, where $\hat{\mathbf{x}} = \mathcal{F}[\mathbf{x}(t)]$, $\hat{\mathbf{f}} = \mathcal{F}[\mathbf{f}(t)]$ and $\mathbf{G}(\omega) = -\omega^2\mathbf{M} + i\omega\mathbf{C} + \mathbf{K}$. The inverse of the matrix $\mathbf{G}(\omega)$ is the nodal transfer function $\mathbf{H}(\omega)$. Hence, the nodal displacements are obtained using $\hat{\mathbf{x}} = \mathbf{H} \cdot \hat{\mathbf{f}}$. The power spectral density (PSD) matrix of the nodal displacements is then determined from the PSD matrix of nodal forces \mathbf{S}^f by $\mathbf{S}^x = \mathbf{H} \mathbf{S}^f \mathbf{H}^*$, where the asterisk indicates the conjugate transpose. The covariance matrix of nodal displacements Σ^x is classically obtained by integration of \mathbf{S}^x . Finally, the covariance matrix of structural response Σ^r is derived from the nodal displacements using the matrix of influence \mathbf{O} , namely $\Sigma^r = \mathbf{O} \Sigma^x \mathbf{O}^T$.

The computational cost of calculations for such a large structure can drastically be reduced operating with a small dimension covariance matrix of modal responses, requiring only the integration of a small number of PSDs of modal displacements. The total displacement consists of two components: a quasi-static (background) term x^B and a resonant term x^R . It has been shown that only the resonant component is well estimated in a reduced modal basis, whereas the quasi-static part requires analysis in a full nodal basis; nevertheless, for the current structure the difference between the results obtained by an analysis developed in modal space and that calculated applying a hybrid analysis are negligible. Since only the covariance matrix is stored during analysis, for each structural member only extreme values of internal forces are known, whereas the information about the instant when such values occur is lost. That is not a problem for the single member, but it can lead to wrong results in computing support reactions, since each connected member reaches its extreme internal force value at a different time. A specific procedure has been developed to prevent the underestimation or, conversely, a drastic overestimation of support reactions and will be discussed in the full paper.

REFERENCES

- EN 1991-1-4, 2010. Eurocode 1 - Actions on structures - Part 1-4: General actions - Wind actions.
Cook, N. and Mayne, J., 1980. A refined working approach to the assessment of wind loads for equivalent static design. *Journal of Wind Engineering and Industrial Aerodynamics* 6, 125–137.
Lawson, T. V., 1976. The design of cladding. *Building and Environment* 11, 37–38.